International Journal of Trendy Research in Engineering and Technology
Volume 10 Issue 5 October 2026
ISSN No. 2582-0958

NONLINEAR AEROELASTIC STABILITY ANALYSIS OF TWO DEGREE OF FREEDOM (DOF) OF AN AIRFOIL

Yared Negussie Alemu
Researcher at Manufacturing Industry Development Institute-Technology and Engineering Industry R& D Center, Addis Ababa, Ethiopia (MTech)
atsedeyared444@gmail.com

ABSTRACT

This paper studies the aeroelastic stability effects of cubic nonlinearities of a two-degree freedom airfoil section that was simplified to a two-dimensional dynamic system with two degree of freedom. The iteration techniques have been performed using merging of p-method is fundamentally a frequency-domain eigenvalue technique designed for linear systems. By using a state-space formulation combined with a time-marching solution we can convert your coupled nonlinear structural equations and aerodynamic states into a first-order system of ordinary differential equations (ODEs). So Runge-Kutta Algorithms (RK4 / RK5) is forwarded for the integration equations of the linear and nonlinear aeroelastic systems with sorts of structural linear and nonlinearities along with flow-type formulations. The data were obtained from the experimental work. This simulation aims to define the flutter zone (dynamic instability boundary) of a 2-DOF airfoil by modeling nonlinearities in both plunge (translational) and pitch (torsional) stiffness. The type of LCO behavior has been examined and used as the main criterion for determining the existence of divergence at the flutter speed. Merging of frequencies will be examined in a linear system and cubic nonlinearities. By evaluating both single-coordinate (e.g., initial pitch only or initial plunge only) and combined-coordinate initial conditions, we are mapping the stable and unstable flutter zone of non-linear dynamic system.

Keywords: Aeroelastic stability effects, Nonlinear systems, Runge-Kutta method, Flutter boundary, Unsteady Flow

1 INTRODUCTION

Small concentrated structural nonlinearity can have significant effects on the flutter behavior and cause large amplitude oscillations at lower airspeeds than for linear and nonlinear systems. So the study of nonlinear effects on structural members is crucial for airfoil stability. When subjected to large aerodynamic forces, that is, airspeed, and an initial plunge distance and pitch angle, the dynamic system can enter an oscillation state. The condition of oscillation of an airfoil that continues to grow out of control is known as flutter. The airspeed at which flutter is induced in a linear aeroelastic system is known as the linear flutter speed. The main focus of this investigation is to study the flutter stability effect of cubic nonlinearities of plunge and pitch stiffness in steady and unsteady flow of an aeroelastic system with two degree of freedom. We also carried out varying parameters of linear and nonlinear characteristics of our problems with variable of velocities, mass, and initial conditions of our aeroelastic problems. So, the structural nonlinearities, the initial conditions of plunge and pitch stiffness with steady and unsteady flow types are critical to select time and frequency marching solution methods. So the simulation result will have discussions on flutter boundary zone of the problems.

Literature Survey

Many works have been investigated in the area of aeroelasticity. The area used by many authors were to get rid of the instabilities of aeroelastic phenomena like flutter and buffeting. The instabilities have been extended to sensitive areas of turbomachinery and control systems of aerospace structure parts. O'Neil and Strganac [1] demonstrated both analytically and experimentally that continuous structural nonlinearities fundamentally change classical flutter into stable limit cycle oscillations (LCOs). Hodges and Pierce [2] in their work, wrote a book that has covered the fundamental mathematical derivation of flutter analysis and also has tried to forward the concept of unsteady aerodynamics. Techniques from nonlinear dynamics and signal processing to the realm of experimental aeroelasticity were developed by Trickey, Virgin, & Dowell [3]. Linear and nonlinear aeroelastic response using a unique test apparatus that allowed for experiments on plunge and pitch motion of a wing with prescribed stiffness characteristics were studied by Block and Strganac [4]. Here, they also examined the addition of a control surface, combined with an active control system, which extended the stable flight region. In their experimental work, unsteady aerodynamics was modeled with an approximation to Theodorsen's theory appropriate for the low reduced frequencies.

Erik Bollt [5] in his work, provided a better understanding of the nonlinear dynamics of the open/closed-loop aeroelasticity of flexible wings with either steady or unsteady aerodynamic loads. He showed that the control could have been effectively suppress Limit Cycle Oscillations (LCO). That could lead to a practical implementation of the control mechanism on actual and future generation aircraft wings via the implementation of a combination of propulsive/jet-type forces. Analysis of this control produced favorable results in the suppression of LCO amplitude and increased flutter boundaries for plunging and pitching motion. The problem of optimizing for steady-state conditions a given nonlinear aeroelastic system by varying both aerodynamic and structural parameters were studied by Maute, Nikbay and Farhat [6]. So, they had made the structure by finite elements and predicted the aerodynamic loads by a three-dimensional finite volume approximation of the Euler equations. They also presented a complete optimization methodology whose key components were a computer-aided geometric design method for representing the design and an analytical approach for sensitivity analysis. Lee, Liu and Wong [7] in their work, advanced the field by pairing implicit finite difference scheme with nonlinear structural equations such as cubic restoring forces to model the behavior of a typical two-dimensional airfoil section, which was focusing only on spring stiffness plunge nonlinearities in their investigations. Also, a secondary bifurcation after the primary Hopf (flutter) bifurcation had been detected for a cubic hard spring in the pitch degree-of-freedom were investigated by Liu and Dowell [8]. Similarly BHK, Price and Wong [9] in their work, different types of structural and aerodynamic nonlinearities commonly encountered in aeronautical engineering were discussed. The aeroelastic stability of a wind turbine rotor in the dynamic stall regime were also investigated by Sarkar and Bijl [10]. The finding of this paper will see the degree of cubic nonlinear types with its unique initial conditions and the solver time-marching techniques that has not been applied in the author's analysis techniques mentioned above.

Scope of the Study

Literature surveys have been investigated from previous researchers. Discussion on p-method forwarded and time marching method of numerical method for nonlinear system have been explained. Concept of aeroelasticity in steady and unsteady flow has been observed. Derivation for linear and nonlinear aeroelastic problem have been forwarded in this work. Matlab code has been performed to find the flutter stability zone of the problems. Simulation has been also performed to see effects of plunge and pitch and mass variables of an airfoil. In addition, the paper will present the result of the comparisons between linear and structural nonlinearities of stiffness in steady flow conditions and also merging the structural nonlinearities with unsteady flow conditions. The topics that will set the future work as it has been forwarded.

FORMULATION OF AEROELASTIC EQUATION

Equations of Motion

In this section, we will demonstrate the flutter analysis of a linear aeroelastic system. Some a flexible mounting system had been developed for flutter tests with rigid wings in wind tunnel [2], [11]. Various aeroelastic systems of idealized and buildup wing structure using gradient based optimization algorism were also demonstrated [6], [12]. Ünal [13] also demonstrated an aeroservoelastic test apparatus is designed to investigate the flutter phenomena in a low speed wind tunnel environment. The flutter analyses were often performed using simple, spring-restrained, rigid wind model such as the one shown in Figure 1.

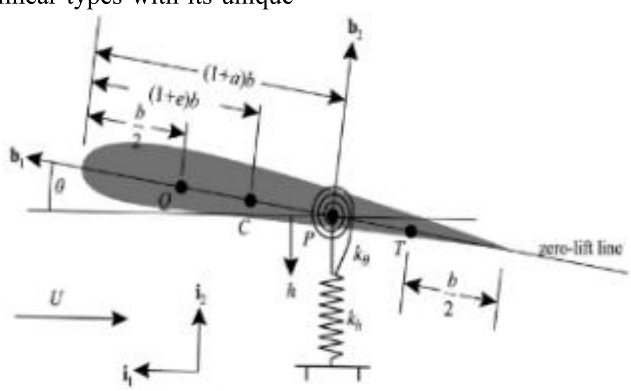

Figure 1 Schematic shows geometry of wing section with pitch and plunge spring restraints

Of interest in such models are points P, C, Q and T which refer, respectively, to the reference point (i.e., where the plunge displacement h is measured), the center of mass, the aerodynamic center (presumed to be the quarter-chord in thin-airfoil theory), and the three quarter-chord (an important chordwise location in thin airfoil theory).

The dimensionless parameter e and a ($-1 \leq e \leq 1$ and $-1 \leq a \leq 1$) determine the location of the points C and P; when these parameters are zero, the points lie on mid chord, and when they are positive (negative), the points lie toward the trailing (leading) edge. In the literature, the chord wise offset of the center of mass from the reference point, rather than e, often appear in the equation of motion. It is typically made dimensionless by the airfoil semi chord b and denoted by $x_\Theta = e - a$. This is so called static unbalance parameter is so positive when the center of mass is towards the trailing edge from the reference point.

The rigid plunging and the pitching of the model is restrained by light, linear springs with spring constants k_Θ *and* k_h. It is convenient to formulate the equations of motion from Lagrange's equations. To do this one needs kinetic and potential energies as well as the generalized forces resulting from aerodynamic loading.

Here, the equation of motion become

$$m(\ddot{h} + bx_\Theta\ddot{\Theta}) + x_h = -L$$

$$I_P\ddot{\Theta} + mbx_\Theta\ddot{h} + x_\Theta = M_{\frac{1}{4}} + b(\frac{1}{2} + a)L \qquad (1)$$

From the steady -flow theory are referred in Anderson's book [14], its use

$$L = 2\pi\rho_\infty U^2\Theta$$

$$M_{\frac{1}{4}} = 0 \qquad (2)$$

Where, in accord with thin airfoil theory, we have taken the lift-curve slope to be 2π. Assuming this representation to be adequate for the time being, we can apply the p method since the aerodynamic loads are specified for arbitrary motion.

To simplify the notation, we introduce the uncoupled, natural frequencies at zero airspeed, defined by

$$\omega_h = \sqrt{\frac{k_h}{m}} \qquad (3)$$

$$\omega_\Theta = \sqrt{\frac{k_\Theta}{I_P}} \qquad (4)$$

We now make the substitutions

$$h = \bar{h}\exp(s\omega_\Theta t) = \bar{h}\exp(vt) \qquad (5)$$

$$\Theta = \bar{\Theta}\exp(s\omega_\Theta t) = \bar{\Theta}\exp(vt) \qquad (6)$$

Where s is an unknown, dimensionless, complex eigenvalue such that $s = \frac{v}{\omega_\Theta}$ which gives

$$\begin{bmatrix} mb^2s^2{\omega_\Theta}^2 + mb^2{\omega_h}^2 & mb^2x_\Theta s^2{\omega_\Theta}^2 + 2\pi{\rho_b}^2U^2 \\ mb^2x_\Theta s^2{\omega_\Theta}^2 & I_P{\omega_\Theta}^2s^2 + I_P{\omega_\Theta}^2 - 2(\frac{1}{2} + a)\pi\rho_\infty b^2U^2 \end{bmatrix}\begin{bmatrix} \frac{\bar{h}}{b} \\ \bar{\Theta} \end{bmatrix} = \begin{bmatrix} 0 \\ 0 \end{bmatrix} \qquad (7)$$

The equation of linear system could be simplified further by using the concept of non-dimensional parameter.

Nondimensional Parameters

It is very convenient to introduce dimensionless variables to further simplify the problem in aeroelastic equations

We let

$$r^2 = \frac{I_P}{mb^2} \qquad \sigma = \frac{\omega_h}{\omega_\Theta}$$

$$\mu = \frac{m}{\rho_\infty}\pi b^2 \qquad V = \frac{U}{b\omega_\Theta} \qquad (8)$$

Where

$r =$ Dimensionless radius of gyration of the wing airfoil about the reference point P with $r^2 \geq {x_\Theta}^2, \sigma =$ ratio of uncoupled bending, $\mu =$ mass ratio parameter reflecting the relative importance of the model mass to the mass of air affected by the model, and $V =$ dimensional free stream speed.

In aerelastic problem of linear or nonlinear type, we face such parameters and so you can apply your mathematical skill to use such dimensionless parameters in aeroelastic systems.

Applying dimensionless variable into Eqs (7) we get the simplified linear aeroelastic equation as

$$\begin{bmatrix} s^2+\sigma^2 & s^2 x_\Theta + \frac{2V^2}{\mu} \\ s^2 x_\Theta & s^2 r^2 + r^2 - \frac{2V^2}{\mu}(\frac{1}{2}+a) \end{bmatrix} \begin{bmatrix} \frac{\bar{h}}{b} \\ \bar{\Theta} \end{bmatrix} = \begin{bmatrix} 0 \\ 0 \end{bmatrix} \quad (9)$$

General linear flutter solution method for this type is called ’p’-method. The definition and solution method are stated in chapter three.

Flutter Boundary

The flutter boundary is usually presented interms of a dimensionless flutter speed as $U_F/(b\omega_\Theta)$. This parameter is similar to the reciprocal of reduced frequency and is called reduced velocity. We can see this parameter in linear flutter speed analysis. Velocity, damping and frequency analysis can be predicted by flutter boundary. Bohbot, Garnier, Toumit, and Darracq [15] also employed adaptive stochastic spectral projection method is to predict limit-cycle oscillations (LCO) of an elastically mounted airfoil with random structural properties.

3 FLUTTER SOLUTION METHODS

The objective of such an analysis is to determine the flight conditions that correspond to the flutter boundary. So we need to see methods of solving the linear and nonlinear problem of aeroelastic equation. Method of solution we are using in this paper is time marching solution method. But we can see first p-method to understand the basics of flutter boundary on this methods.

Linear Flutter Solution method

It has been applied in brief in [16], [17]work to solve flutter boundary of linear aeroelastic system. Non-steady Euler equations are coupled with a typical section swept wing model and integrated forward in time marching were explained [18].The point here is that we need to first solve the nontrivial solution of aeroelastic equation by setting the zeroes of the determinant of the problem. The solution of the generalized equations of motion for the displacement $w(x,y,t)$ normal to plane of the model in Section 2.2 with aerodynamic coupling can be written as

$$\mathrm{w(x,y,t)} = \sum_{k=1}^{2} q_k(x,y)\exp[(\Gamma_k + i\Omega_k)t] + \bar{q}_k(\mathrm{x,y})\exp[(\Gamma_k - \mathrm{i}\Omega_k)\mathrm{t}]\} \quad (10)$$

We note that Parameters can be stated as follows:

k = 1 for plunge mode, k = 2 for pitch mode

The conjugate pair could be set as $v_k = \Gamma_k \pm i\Omega_k$

Γ_k is modal damping of the kth mode

Ω_k is modal frequency of the kth mode

We note here that the solution has been used to solve the set of second-order, linear, ordinary differential equations. It has been used for two degree system of our type. But we can extend the solution from two degree freedom to more than two degree of freedoms as well.

Since the equation is described by mode shapes of conjugate complex parameter v_k, the differential equations are homogeneous and is a function of a simple exponential time. With this ground, we can note that the general coordinate system as

$$q_k = \bar{q}_k \exp(\mathrm{vt}) = \bar{q}_k \exp(s w_\Theta\, t) \quad (11)$$

Where s is an unknown, dimensionless complex eigenvalue.

We seek here to solve only the two degree freedom of aeroelastic problem. So the plunge and pitch coordinates limit our model of Section 2.1. From the p solution method of conjugate complex method, we first need to change the equation in nondimensional standard parameters that was forwarded in Section 2.2.

Our nonlinear aeroelastic problems can also be solved by numerical analysis of Rungekutta method. So we will apply the time domain and the frequency domain solution methods in the next chapters. The aeroelastic system that is modeled consisted of a two-dimensional airfoil in a free stream of air with restoring forces in both the plunge and pitch degrees of freedom. This system can be schematically represented in Figure 1. And by modifying the stiffness to cubic nonlinearity, our model will be studied.

Aerodynamically, the lifting forces are determined from thin airfoil theory where the coefficient of lift is 2π. The damping coefficients for the system are neglected throughout the analysis of the system equations. In unsteady flow, we will face damping action in the system equations and also the lift and the pitching moment will be taken from the Theodorsen's Unsteady Thin-Airfoil concept as it has been forwarded in chapter five.

Time Marching Solution for Numerical Analysis

Basically we seek to find the time history of the equation of nonlinear equation. So it is common to find step by step numerical method of solving nonlinear problems. In particular, given the motion at some time, t, we wish to be able to obtain the motion at some later time,t + Δ. In relating the solution at time, t + Δ, to that at time, t, we use the idea of a Taylor series. And we could get more exact answer as we include more order of differential equation in the equation. The built function ode 45 code in matlab can do such task through integration up to 4th and 5th order. The response of the system is simulated, subject to a set of given initial condition and in this case mainly the initial pitch angle and airspeed were varied to produce a response of the system with time in each of the degrees of freedom.

Here is the simulation computed until the system response either damped out to zero, diverged beyond acceptable bounds. Mass effect has also been analyzed in the simulation to see the effects of stability of the system. The results of each simulation were then evaluated to determine which of the three conditions resulted:

1. Damped oscillations (stable): the oscillations of the system die out over time such that the amplitude of the system reached approximately zero and no further motion is present.

2. Divergent oscillations (unstable): the oscillations of the system grow beyond the bounds of the simulation and the system is deemed to have become unstable.

3. Limit cycle oscillations (LCO) the oscillations tend neither to damp out to zero nor to grow to infinity but rather become self-sustained at an amplitude of some intermediate value. This result was determined to be a limit cycle response.

As we go through papers we can observe continuous load disturbance due increasing the airstream velocity as shown in Figure 2.

In our model we haven't consider the damped case in the solution of linear and nonlinear types of steady flow. So we will see aerodynamic effect in the unsteady flow for damping action to be take place and get what we will expect of the two motion in Figure 2.

Note that the time history of the undamped response has a certain well defined average period or frequency with modulated, constant amplitude. The frequency marching solution has been evaluated using FFT method.

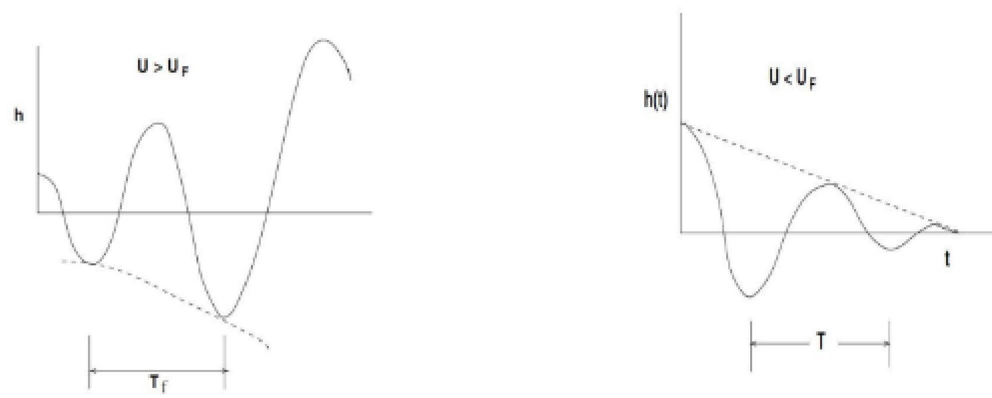

(a) Time history of unstable motion

(b) History of stable motion

Figure 2 Time history of flutter boundary-(a) and (b)

State Space Equations The linear and nonlinear model can be designed by adding all lower derivatives with time in state space forms: $(\ddot{q} = \dot{q},\ q, t)$. So models have been developed using this formulation in our linear and nonlinear system.

where the two degree freedom generalized form is due to h and θ.

Limit Cycle Oscillation

Limit cycle oscillation can be regarded as equilibrium motion in which the system performs periodic motion, as opposed to equilibrium points in which the system is at rest. Moreover the amplitude of a given cycle depends on the system parameters alone. The simulation results could be analyzed using output of time marching solution.

Frequency Domain Solutions

An alternative procedure to the time domain approach is to treat the problem in the frequency domain. This approach is more popular and widely used today than the time domain approach. Perhaps the most important reason for this is the fact that the aerodynamic theory is much more completely developed for simple harmonic motion than for arbitrary time dependent motion. Another reason for the popularity of the frequency domain method is the powerful power spectral description of random loads such as gust loads, landing loads (over randomly rough surfaces), etc. These require a frequency domain description. The principal disadvantage of the frequency domain approach is that one performs two separate calculations; one, to assess the system stability, flutter, and a second, to determine the response to external loads such as gusts, etc. Only the harmonic solutions have been considered in our model for evaluating the signals by FFT.

4.AIRFOIL WITH STIFFNESS NONLINEARITIES

Many investigators have considered such a configuration with a variety of nonlinear stiffness modes. Unsteady flow analysis to investigate a 2D unsteady viscous solver of an airfoil to analyze a standard linear or non-linear state-space formulation were also examined [19]. Reddy, Srivastava and Mehmed [20] in their work, analyses flutter and forced response for a cascade of blades in subsonic and transonic flow. In general, good quantitative correlation was found for simple wind tunnel models and the basic physical mechanism that led to LCO appears well understood in Texas team work [1].

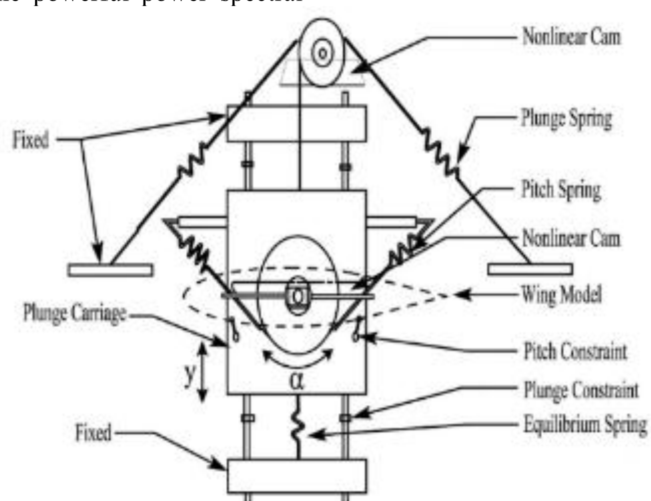

Figure 3 Typical experimental work for bilinear stiffness

Here, they had conducted experiments with their nonlinear aeroelastic test apparatus in a low speed wind tunnel, and these investigations of typical section models provided validation of their theoretical models. See Figure 3. The testbed has been used to investigate both linear and nonlinear responses of wing sections as well as the development of active control methods. Nonlinear aeroelastic analysis of high-aspect-ratio flexible wings were conducted [21].Figure 3 also shows the parameters involved on the model.

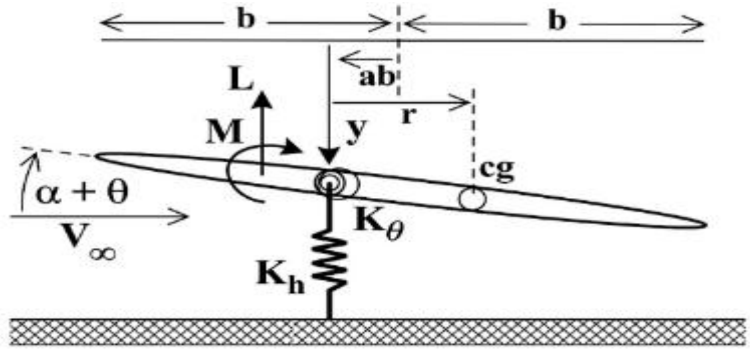

Figure 4 Aeroelastic system is modeled by a rigid wing section attached to a flexible support that permits pitch and plunge motion

Where parameters are defined as follows:

b: Half-chord length of the airfoil

ab: Distance from the mid-chord to the elastic axis/pivot point

r or x_a : Distance from the elastic axis to the center of gravity (cg)

K_h / K_Θ : Plunge and pitch stiffness springs

L / M: Aerodynamic Lift force and Pitching Moment

Their experiments with freeplay nonlinearities showed that LCOs at freestream velocities was less than the linear flutter velocity. The LCO amplitude grew with an increase in freestream velocity until the flutter occurred at the linear flutter velocity. Further investigations showed two LCO amplitudes that depended upon the initial condition at the same freestream velocity.

Necessary data for cubic nonlinearities of our model are taken from such model. Physical properties of the experiment hardware and associated analyses are provided next: $a = -0.450$; m_T =10.3 kg ; m_W=1.662 kg;

b = 0.1064m; span s = 0.6m; airfoil profile= NACA0012; $K_\Theta = 2.57$; N-m/rad (linear case) and K_h=2860N/m (linear case).

Approaching the Flutter Boundary

For low speed (incompressible flow) flutter tests, the flutter boundary were normally approached by increasing the flow velocity in suitable increments [1]. This work had been conducted to show the limit cycle oscillation (LCO) of the plunge and pitch motion in this nonlinearity. In time marching simulation result shows that the motion starts to diverge at flutter speed.

Here in our model we are demanding structural nonlinearities by modifying the linear stiffness constant into cubic nonlinearities. and we don't have damping force in the structural parts. So we will analyze the energy equations to study about mode shape created in harmonic motion or periodic motion before flutter has been created.

Here, we can take the modified part as:

$k_h(1 + 0.01h^3)$ and $k_\Theta(1 + 0.01\Theta^3)$ for the plunge and pitch stiffness respectively.

After rearranging the equations of potential energy and kinetic energy of aeroelastic systems as we have done in section 2.1 we will get the following equation.

$$m(\ddot{h}+bx_\Theta\ddot{\Theta}) + k_h h + \left(\frac{k_h h^4}{40}\right) = -L$$

$$I_P\ddot{\Theta} + mbx_\Theta\ddot{h} + K_\Theta\Theta + \left(\frac{K_\Theta\Theta^4}{40}\right) = M_{\frac{1}{4}} + b\left(\frac{1}{2} + a\right)L \quad (12)$$

We could take the lift and pitching moment coefficient from the steady flow theory and putting them into the Eqs. 12. Or applying the same procedure we have applied in Eqs. 9, the expected matrix formulation will be

$$\begin{bmatrix} mb^2 & mb^2x_\Theta \\ mb^2x_\Theta & I_P \end{bmatrix}\begin{bmatrix} \frac{\ddot{h}}{b} \\ \ddot{\Theta} \end{bmatrix}+\begin{bmatrix} mb^2 & 2\pi\rho_\infty b^2U^2 \\ 0 & I_P\omega_\Theta{}^2-2(\frac{1}{2}+a)\pi\rho_\infty b^2U^2 \end{bmatrix}\begin{bmatrix} \frac{h}{b} \\ \Theta \end{bmatrix}+\begin{bmatrix} \frac{\omega_h{}^2mb^2}{40} & 0 \\ 0 & \frac{\omega_\Theta{}^2I_P}{40} \end{bmatrix}\begin{bmatrix} \frac{h^4}{b} \\ \Theta^4 \end{bmatrix}=\begin{bmatrix} 0 \\ 0 \end{bmatrix} \quad (13)$$

If the mass involving in the kinetic energy of the airfoil is due to two different mass of plunge and pitch constraints, we will have the relation shown in Eqs. 1. The mass in plunge is always greater than the mass involved in pitch constraint since the plunge constraint supports the mass involved in the systems. Consider the point mass involving for the plunge constraints be m_p and similarly point mass due to pitching constraints be m_ω. In our similar models of Figure 1 and Figure 3, the total mass is subjected to be carried on plunge springs. So we can make analysis on different masses involved in the two constraints. To study on mass balancing in the design of aircraft structure is fundamental science in the aeroelastic stability of the system.

$$\begin{bmatrix} m_pb^2 & m_\omega b^2x_\Theta \\ m_pb^2x_\Theta & I_P \end{bmatrix}\begin{bmatrix} \frac{\ddot{h}}{b} \\ \ddot{\Theta} \end{bmatrix}+\begin{bmatrix} m_pb^2 & 2\pi\rho_\infty b^2U^2 \\ 0 & I_P\omega_\Theta{}^2-2(\frac{1}{2}+a)\pi\rho_\infty b^2U^2 \end{bmatrix}\begin{bmatrix} \frac{h}{b} \\ \Theta \end{bmatrix}+\begin{bmatrix} \frac{\omega_h{}^2m_pb^2}{40} & 0 \\ 0 & \frac{\omega_\Theta{}^2I_P}{40} \end{bmatrix}\begin{bmatrix} \frac{h^4}{b} \\ \Theta^4 \end{bmatrix}=\begin{bmatrix} 0 \\ 0 \end{bmatrix} \quad (14)$$

Solving in time marching solution needs to be arranged in state space form. To solve the state space of the above nonlinear problem we should do the following procedure

1. Separate the variables of $\frac{\ddot{h}}{b}$ and $\ddot{\Theta}$ from the Eqs.14.

2. Formulate the variables in step one into the form $\ddot{h} = (\dot{h}, \dot{t})$ and $\ddot{\Theta} = (\dot{\Theta}, t)$

3. Combine the variables in step two into four state space form of equations.

4. We use the time marching solution method of Runge Kutta numerical analysis to make integration of the system. ODE 45 matlab code has been applied to solve such problem. The FFT result have been also analyzed using matlab code. In this section, we will study aeroelastic system of linear and nonlinear stiffness problems in steady aerodynamic flow parameters. The simulation results have been done first for linear structural stiffness matrix and next for cubic nonlinearities structural stiffness matrix. This is to compare the results of the two cases.

We have performed three simulations on linear stiffness shown bellow. To do this we have followed the above procedure in section 4.2 to simulate for kinds of initial condition problems. The expected result will show merging of frequencies of flutter speed. Also eroelastic response for pure plunging motion of a typical section were also presented [22].

The amplitude of coupled frequency would be also higher than the uncouple frequencies. The dependency on initial condition will be also realized in the system equations.

Simulation done and discussion on linear structural Stiffness in Steady Flow:

Cases have been assigned in the figures below for types of initial condition taken for case linear stiffness

Case (a) is for linear stiffness with initial condition of 0 meter and 0.26 rad constraints case linear stiffness

Case (b) is for linear stiffness with initial condition of 0.01 m plunge and 0 rad constraints case linear stiffness

Case (c) is for linear stiffness with initial condition of 0.01 meter and 0 rad constraints of the same mass effect

Simulation done using the initial condition of 0 m plunge and 0.26 rad pitch or Case (a)

The equivalent value of 0.26 is equal to 15 degree. So it has been large initial condition in this simulation. (b)

Figure 5a shows the limit cycle oscillation at the critical flutter speed of 5.8m/s. The shooting frequency value is 2.5hz as shown in Figure 5b. No damping action has been seen in structural equation of the system. The oscillation type before the flutter speed was periodic. It had been investigated.

ISSN No. 2582-0958

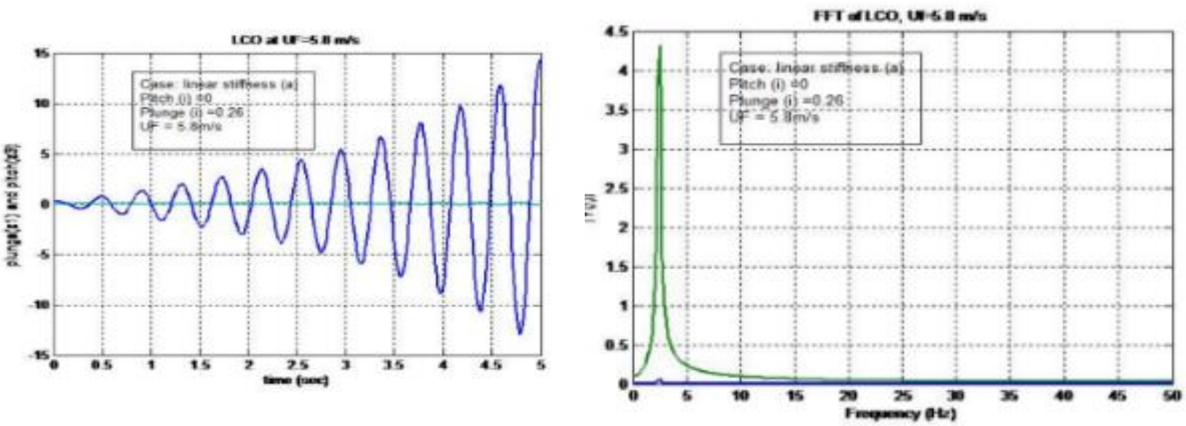

(a) (b)

Figure 5 Limit cycle (a) and FFT (b) values of linear stiffness at 0.01 m plunge and 0.26 rad pitch that the harmonic motion was due to no damp

The uncoupling frequencies of the plunge and pitch mode before the flutter speed and the coupling frequencies after the flutter speed is common in this flutter analysis. The amplitude of the signal is 4.3 at the flutter speed. The number of cycle in the plunge and the pith are the same. Here the coupling effect is continuously observed in the flutter zone (upto complete divergence lasts in the oscillation).

Simulation result for 0.01 m plunge and 0 rad value for linear structural value in steady flow or Case (b)

The simulated result has been shown in the Figure 6.The damping action is not recorded in the equation. So the periodic oscillation before flutter and the divergent type after the flutter point will be observed in the simulation result. The coupling frequency is observed at flutter speed of 5.8 m/s and the resulting frequency is 2.5 Hz. The number of cycle in the flutter zone for the pitch and plunge mode is same with case (a) as it has been observed the time domain marching solution. Continuously merging of frequency is observed in the system after the flutter speed.

The same mass effect in case(c) mean that we have same mass components in plunge and pitch constraints. Here we have chosen, say, the small mass involved in pitch constraint and substitute this mass for the plunge mass which is mentioned in section 4.1 as m_{ω}=1.662 kg. The test has been presented for which the mass involved here is from standard NACA0012 of section 4.1. Flutter speed has been increased to 21.9m/s. Here is the result shown in Figure 7. Generally we will get higher pitch amplitude than the plunge amplitude.

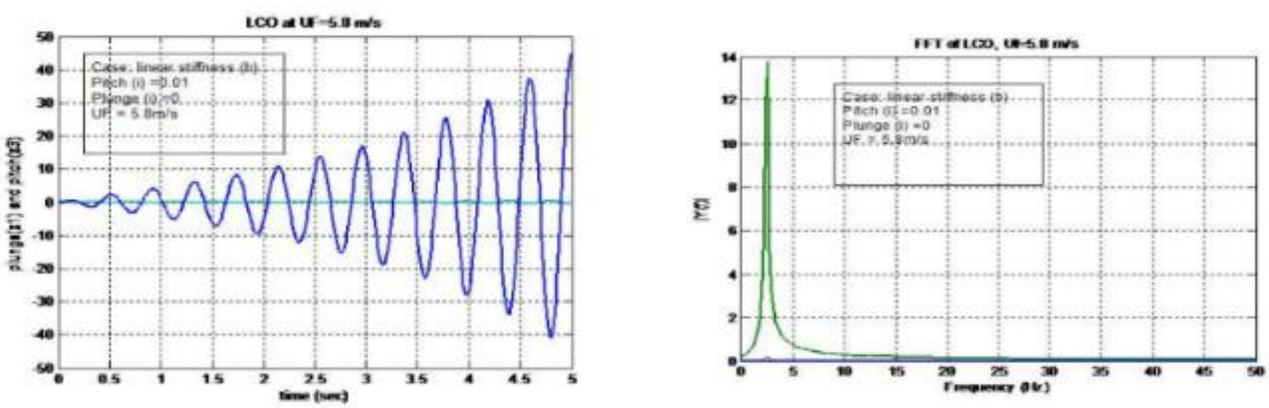

(a) (b)

Figure 6 Limit cycle (a) and FFT (b) values of linear stiffness at 0.01 m plunge and 0 rad pitch

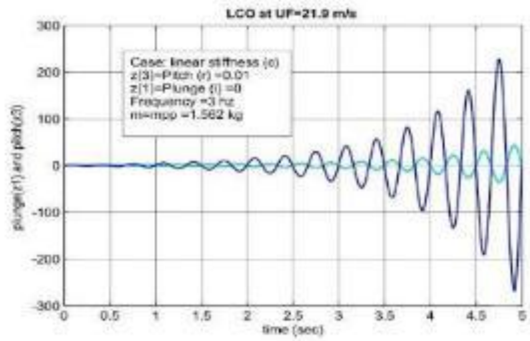

(a)

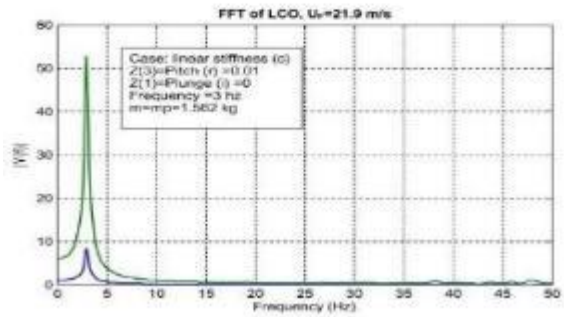

(b)

Figure 7 Limit cycle (a) and FFT (b) values of linear stiffness at 0.01m plunge and 0 rad pitch of the same mass effect

So by formulating mass substitution of shown above, we will get higher flutter speed and higher frequency magnitude.

In all three figures, Figure 5, Figure 6 and Figure 7 the uncoupling before the flutter speed and coupling of 2.5 is observed at FFT simulation of the above mentioned figures and this is what we have expected from the simulation result.

Table 1 summarizes the simulation outcomes for structural stiffness under steady flow conditions, detailing what was covered in section 4.2.

Table 1 Summery on Simulations result for structural stiffness in steady flow

Case	Range Of Flutter	Mass Effect		Initial Condition		Flutter Speed M/S	Excitation Frequency from FFT figure HZ	Convergence	Coupling Of Frequency	Amplitude read from FFT figure
		Plunge Kg	Pitch Kg	Plunge m	Pitch rad					
Figure 5	$U < U_F$	10.3	1.662	0	0.26	5.8	2.5	Periodic	No	4.3
	$U > U_F$							Diverge	High	
Figure 6	$U < U_F$	10.3	1.662	0.01	0	5.8	2.5	Periodic	No	13.8
	$U > U_F$							Diverge	High	
Figure 7	$U < U_F$	1.662	1.662	0.01	0	21.9	2.5	Periodic	No	54
	$U > U_F$							Diverge	High	

Simulation Done and Discussion on Nonlinear Structural Stiffness in Steady Flow

We will perform three simulations using initial conditions used in the previous section. In this linear flutter analysis we have seen the merging of frequencies at all initial conditions of the problems. Papers have been done also on the coupling of frequencies on system with single nonlinearity of plunge or pitch constraints. The work are now modeling the system based on thethe case et here so that coupling behavior of flutter at the flutter speed il be investigated. In addition we will test the range of flutter speed in the nonlinearities as we compare with the linearity.

Designation has been set here for the subsections and figures shown below like we did in the above section 4.2.

Case nonlinear stiffness (a) is for nonlinear stiffness with initial condition of 0 meter and 0.26 rad constraints

International Journal of Trendy Research in Engineering and Technology
Volume 10 Issue 4 August 2026
ISSN No. 2582-0958

Case nonlinear stiffness (b) is for nonlinear stiffness with initial condition of 0.01 meter and 0 rad constraints

Case nonlinear stiffness (c) is for nonlinear stiffness with initial condition of 0.01 meter and 0 rad constraints of the same mass effect

Case nonlinear stiffness (d) is for 0.01 m plunge distance and 0.26 rad pitch angle.

Simulation done using the initial conditions of 0 m plunge and 0.26 rad pitch or Case nonlinear stiffness (a)

As the speed become near to flutter point, the behaviors of random oscillation resulted in as shown in Figure 8 Plunge mode shape at (a) and Pitch mode shape (b) for initial conditions of 0 m plunge and 0.26 rad pitch are also depicted in this figure. Also we observe that the flutter mode reply are commenced at a speed of flutter velocity (UF = 5.8 m/s) for those initial conditions plunge and pitch of this section.

Also in Figure 9 FFT of modes (a) and LCO at U < UF (b) of 0 m plunge and 0.26 rad pitch, the system excitation frequencies are concentrated at the last bound of flutter zone. Or ranges of frequencies are liable to unstable conditions at such finishing time of flutter bound. Mode b of this figure shows that mode shape is periodic before the flutter speed, i.e. 5.5m/s. As the speed become near to flutter point, the behaviors of the LCO become random oscillation as shown in figure 8. The magnitude of amplitude could be analyzed from the figure. Close to the final bound time of LCO, the uncoupling of frequencies has been observed. This is different from the linear system shown in section 4.2. Hence time limit has been considered for the uncoupling of frequencies. The shapes of the two modes are the same at this final bound of flutter point. The number of harmonic cycle shown in Figure 8 is same. The magnitude of pitch signal is much higher than the plunge signal. This is why the plunge signal is very close to the reference line.

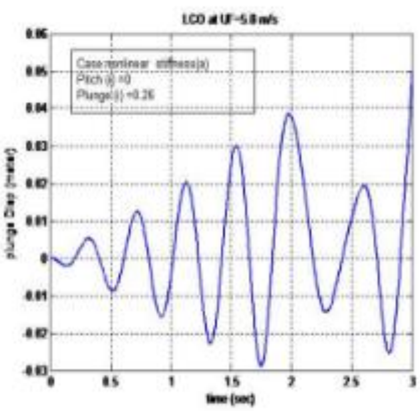

(a)

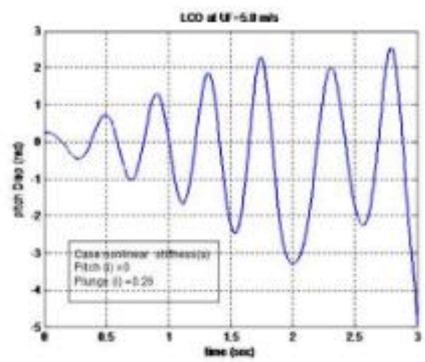

(b)

Figure 8 Plunge mode shape at (a) and Pitch mode shape (b) for initial conditions of 0 m plunge and 0.26 rad pitch

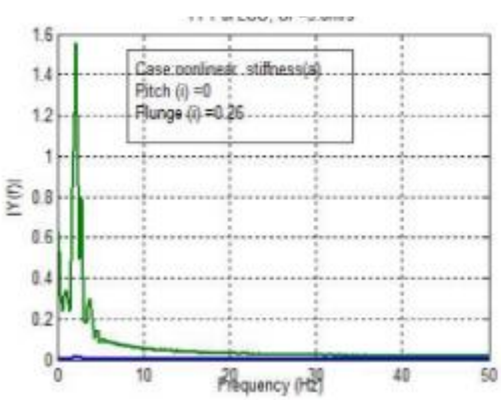

(a)

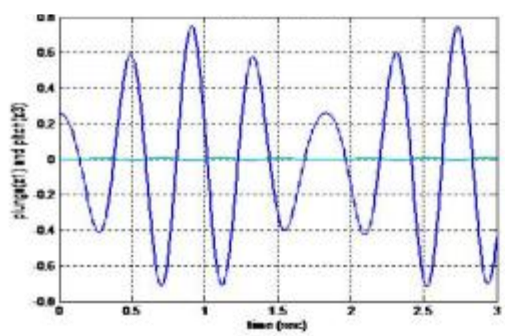

(b)

Figure 9 FFT of modes (a) and LCO at U < UF (b) of 0 m plunge and 0.26 rad pitch

Simulation done using the initial condition of 0.01 m plunge and 0 rad pitch or Case nonlinear stiffness (b)

Here in Figure 11a two peak frequencies dominate the other small frequencies at the final bound of flutter speed, i.e.5.6m/s. So the coupling of frequencies will not be observed in this specified initial value problem at this final bound of flutter speed. A computational method for flutter prediction of turbomachinery cascades were presented [3]. The flow through multiple blade passages was calculated using a time-domain approach with coupled aerodynamic and structural models [23]. The periodic motion that have been considered before onset of the flutter point as shown in the Figure 10a and Figure 10b, of two mode shapes at the speed of 5.5m/s. The two peak excitation frequencies will be shown at 2 and 2.6 Hz. The result shows that the shapes of modes are different. Limit cycle time bound have been considered in section 4.5.1 to analyze coupling of frequencies. So having simulation result at the onset of time bound of flutter zone, we could analyze the merging of the two frequencies to each other. Note that the coupling frequencies are the two peak frequencies.

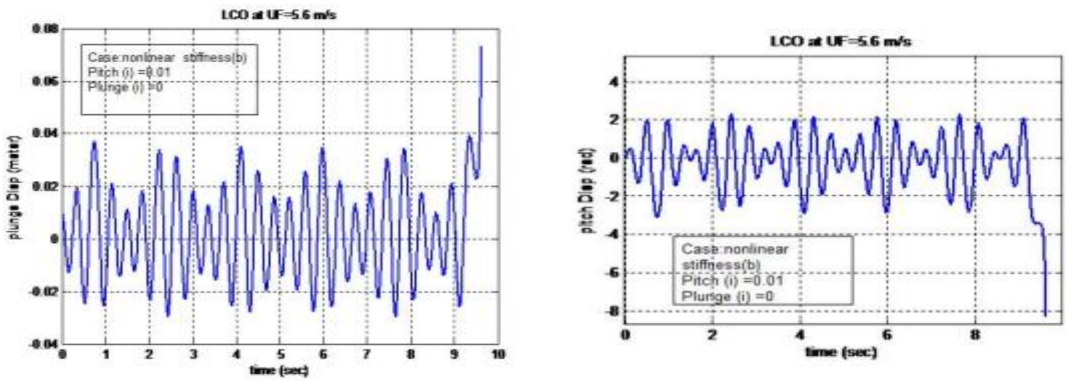

(a) (b)

Figure 10 Plunge mode (a), Pitch mode (b) of 0.01 m plunge and 0 rad pitch

Approaching of signal for range of time signal has been observed towards the final bound of flutter zone. And the shape of the LCO we have tested in case nonlinear (a) and here, case nonlinear (b), is different. Total time to get flutter speed is 9.6 sec in this simulation. So time taken we observed in case nonlinear (a) is less than here in case nonlinear (b). Here the smallest time taken for evaluating the signal is 0.01 sec in the FFT analysis. The time taken for flutter test depends on the behavior of the system initial conditions. The shape of the LCO we have tested in case nonlinear (a) and case nonlinear (b) is different.

Here the time taken to get the flutter speed is 9.6 second. In this simulation the time to get flutter speed will take longer time than the condition taken in case linear (a). Note that the smallest interval taken for time integration is 0.01sec throughout this work.

Simulation result for the same mass effects for nonlinear stiffness in steady flow or Case nonlinear stiffness (c)

We have seen effects of the nonlinearities on the flutter speed in section 4.5.1 and section 4.5 2. The simulation result shows the response of the system is dependent on the initial condition of the system. The periodic shape and the behavior of uncoupled frequencies would be observed before flutter point in Figure 12 . The mode shape of the two signals is also different to each other at the onset and final LCO of the system. Hence the behavior of the system here is different from the above simulation results that have seen in section 4.5.1 and section 4.5.2.

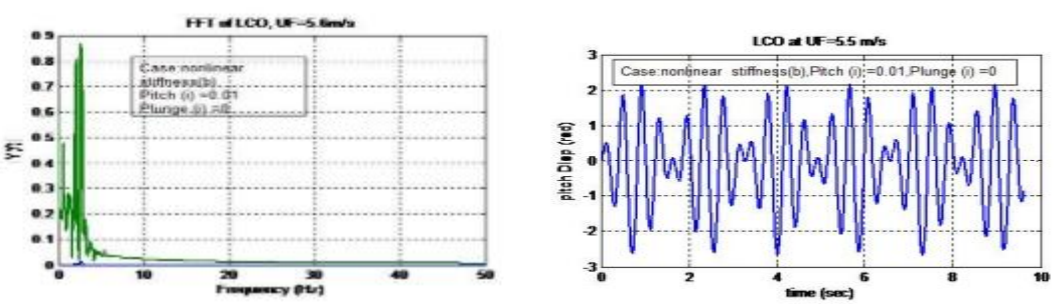

(a)

(b)

Figure 11 FFT of modes (a) and LCO at U < UF (b) of 0.01 m plunge and 0 rad pitch

Here by adding modification on plunge mass parameter without changing the mass of NACA0012 airfoil structural setup, we could analyze the same mass effect on the two degree freedom of a system. The result of the simulation shown in Figure 13 have been tested at the flutter speed of 21.7 sec. Here the two peak frequencies are at 2.5 and 3.5Hz. The simulation result shows also the two peak frequencies are a bit far from each other.

Simulation result for 0.01 m plunge distance and 0.26 rad pitch angle value of nonlinear stiffness or Case nonlinear stiffness (d)

By simulating the above coordinate we could compare the result here with that of done in section 4.5.1 and section 4.5.2. The results of the simulations are shown in the Figure 14 and (a) (b)

Figure 15.

Here the coupling of frequencies will be more pronounced as both initial conditions comes into action. This point the amplitude of frequencies will be greater than the system, where single initial condition comes to exist in the simulation result as shown in Figure 9a and Figure 11a.

Generally we can come to the point that as we give more coordinate to the system, the flutter speed will decrease and the amplitude will also increase at the same time. As shown in table 4.1, the couplings of the frequencies are taking place in the flutter zone which supports the suggestion given above. Here the two frequencies parameter will be come near to other at the flutter zone. This has been tested in the coordinate parameter of section 4.5.4 and summarized in

Table 2.

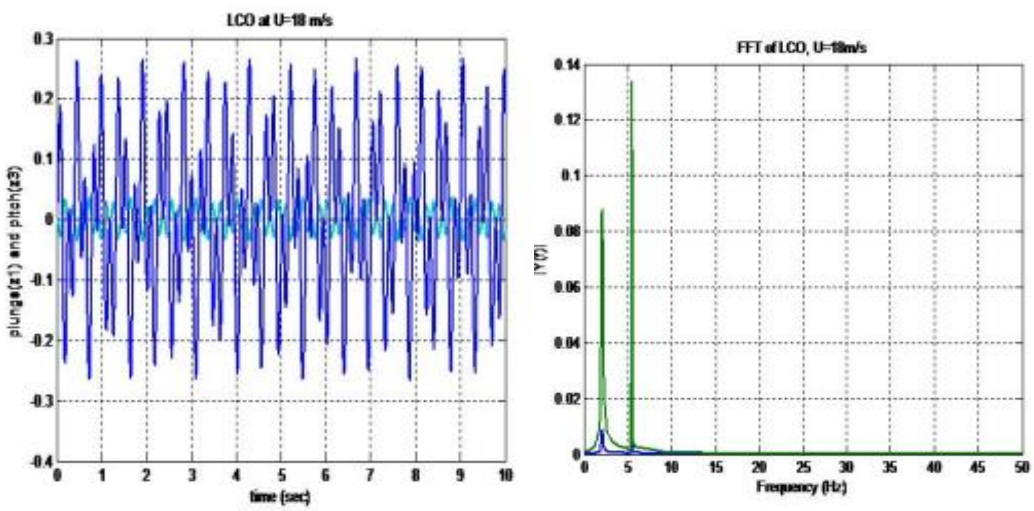

(a) (b)

Figure 12 Plunge mode (a), Pitch mode (b) of 0.01 m plunge and 0 rad pitch

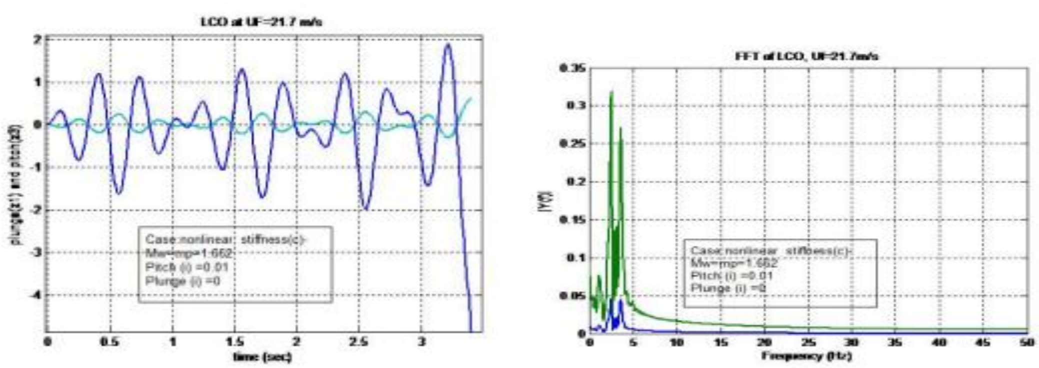

(a) (b)

Figure 13 FFT of modes(a) and LCO at U > UF (b)of 0.01 m plunge and 0 rad pitch of same mass effect

ISSN No. 2582-0958

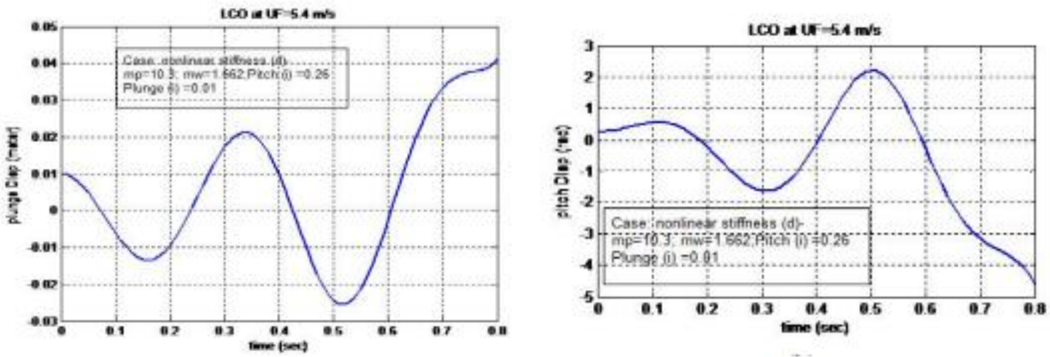

(a) (b)

Figure 14 LCO of plunge (a) and LCO of pitch (b) for both given initial constraints

Table 2 The coupling effect of frequencies by increasing velocity

U in m/s	frequency(1)	frequency(2)
1	1.76	3.5
3	1.85	3.32
5	2.05	2.92
5.4	2.5	2.5

The amplitude of 2.3 magnitude in pitch FFT result that are shown in the Figure 15a are greater than the magnitude shown in case nonlinear (a) in the Figure 9a and case nonlinear (b) as shown in Figure 11a. The flutter speed is 5.4 which is less than what we have seen in section 4.5.1 and 4.5.2. The plunge and the pitch mode is shown in Figure 14 which has only short period time interval to get flutter.

On the other hand the coupling phenomenon is observed at 2.5 Hz. Coming to the Table 2, the uncouple frequencies is shown before the flutter point and the range of approaching is from the two sides to get the system flutter point.

The sensitivity of flutter speed is so generally the behavior of LCO of the two plunge and pitch signal at which the system starts to diverge

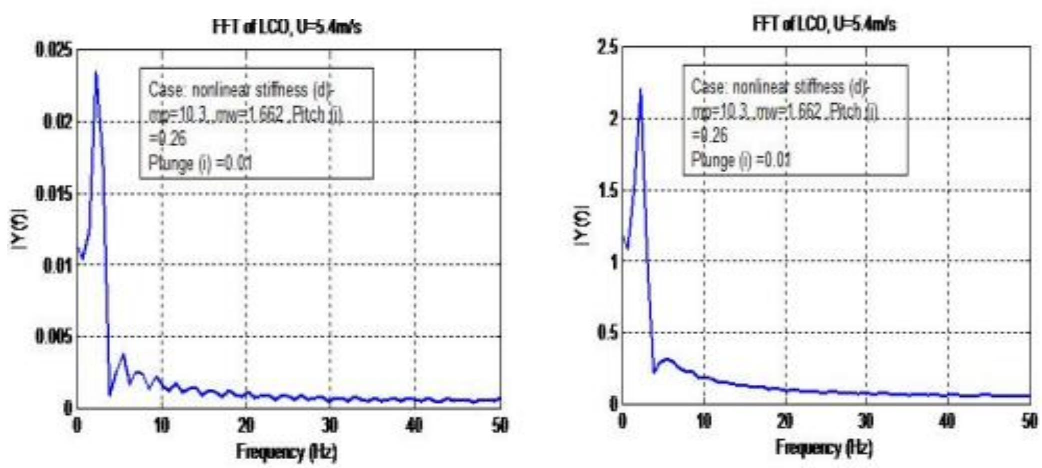

(a) (b)

Figure 15 FFT of plunge (a) and FFT of pitch(b) for both nonlinearities with the given both initial constraints

Summary of the nonlinear stiffness simulation in steady flow have been illustrated in

Table 3. The table shows how the nonlinearity decreases the flutter speed as we compare the result with the linear cases. The couplings of frequencies have been considered for two peak frequencies in all cases of the simulation.

The periodic motion is common for the airstream velocity below flutter speed. How the initial conditions influence the flutter speed could be observed in this table.

The frequency value is taken for the final bound of simulation result. This doesn't mean that the systems don't have coupling effect at the flutter zone. So we could see more coupling effect for cases of the simulation result before the two peak frequencies.

Table 3 Summery on nonlinear stiffnesses for the given intial condtions

Case	Range Of Flutter	Mass Effect		Initial Condition		Flutter Speed	Excitation Frequency	Convergence	Coupling Of Frequency	Amplitude
		Plunge Kg	Pitch Kg	Plunge m	Pitch rad	M/S	HZ			
Figure 16	$U < U_F$	10.3	1.662	0	0.26	5.8	2.0	Periodic	No	----
Figure 9	$U > U_F$							Diverge	High	1.6
Figure 10	$U < U_F$	10.3	1.662	0.01	0	5.6	2,2.6	Periodic	No	---
Figure 11	$U > U_F$							Diverge	High	0.9
Figure 12	$U < U_F$	1.662	1.662	0.01	0	21.7	2.5,3.5	Periodic	No	---
Figure 13	$U > U_F$							Diverge	High	0.9
Figure 14	$U < U_F$	10.3	1.662	0.01	0.26	5.4	2.5	Periodic	No	---
Figure 15	$U > U_F$							Diverge	More	2.3

5 NONLINEAR AEROELASTIC ANALYSIS IN UNSTEADY FLOW

In chapter two and chapter four, flutter analysis was conducted using aerodynamic theory in steady flow. The lift and pitching moment used were functions only of the instantaneous pitch angle, θ. In a more complete unsteady aerodynamic theory, the left and the pitching moment consists of two parts from two physically different phenomena: noncirculatory and circulatory effects. To manage the Hopf bifurcation and achieve desirable nonlinear dynamics, other authors tried also used Normal Form of Hopf Bifurcation [24].

Noncirculatory effects, also called apparent mass and inertial effects, are generated when the wing motion has a nonzero acceleration. It has to be then carry with it a part of the air surrounding it. That mass has finite mass, which leads to inertial force opposing its acceleration.

Circulatory effects are generally more important in aircraft wings. Indeed, in steady flight it is the circulatory lift that keeps the aircraft aloft. Vortices are an integral part of the generation of circulatory lift.

Concept of Unsteady Thin-Airfiol Theory

Theoderson conducted a theory of unsteady aerodynamics for a thin airfoil undergoing small oscillations in compressible flow. The lift contains both circulatory and noncirculatory terms, where as the pitching moment about the quarter-chord is entirely noncirculatory. The lift and the pitching moments are given by

$$L = 2\pi\rho_\infty UbC(k)\left[\dot{h} + U\Theta + b\left(\frac{1}{2} - a\right)\dot{\Theta}\right] + \pi\rho_\infty b^2(\ddot{h} + U\dot{\Theta} - ba\ddot{\Theta})$$

$$M_{\frac{1}{4}} = -\pi\rho_\infty b^3\left[\frac{1}{2}\ddot{h} + U\dot{\Theta} + b\left(\frac{1}{8} - \frac{a}{2}\right)\ddot{\Theta}\right] \quad (15)$$

Where $\rho_\infty$is the density of air, Theodorsen $C(k)$is a complex valued function and k is the reduced frequency (ωU/b). The exact expression is C(k) of the form

$$C(k) = F(k) + iG(k) \quad (16)$$

Where $F(k)$ is real part of $C(k), iG(k) is\ imaginary\ parts\ of\ C(k)$

Usually the exact Theodorsen function is not used directly, but it is replaced by approximate functions

$$C(k) = 1 - \frac{0.165}{1-i\frac{0.0455}{k}} - \frac{0.0335}{1-i\frac{0.3}{k}} \quad (17)$$

Aerelastic Equations in an Unsteady Flow

To start solving the equation of motion, we take Lagrange's equations of motion Eqs **Error! Reference source not found.** in chapter two and replace the lift and piching moment of Eqs (15) in the right side of the Eqs (2). By collecting coefficient matrix of same type in structural part ,The negative of the lift and momentum equations can be formulated as

$$\begin{bmatrix}-L\\ M\end{bmatrix} = \begin{bmatrix}-\pi\rho b^2 & \pi\rho b^3 a\\ \pi\rho b^3 a & -\pi\rho b^4(\frac{1}{8} + a^2)\end{bmatrix}\begin{bmatrix}\ddot{h}\\ \ddot{\Theta}\end{bmatrix} + \begin{bmatrix}0 & -\pi\rho b^2 U\\ 0 & -\pi\rho b^3 U(\frac{1}{2} - a)\end{bmatrix}\begin{bmatrix}\dot{h}\\ \dot{\Theta}\end{bmatrix} +$$

$$2\pi UbC(k)\left(\begin{bmatrix}-1 & -b\left(a + \frac{1}{2}\right)\\ b\left(a + \frac{1}{2}\right) & b^2\left(a + \frac{1}{2}\right)\left(\frac{1}{2} - a\right)\end{bmatrix}\begin{bmatrix}\dot{h}\\ \dot{\Theta}\end{bmatrix} + U\begin{bmatrix}0 & -1\\ 0 & b(a + \frac{1}{2})\end{bmatrix}\begin{bmatrix}h\\ \Theta\end{bmatrix}\right) \quad (18)$$

The lift and moment for incompressible subsonic flow can be separated into two parts; circulatory and non-circulatory Eqs (18). As stated earlier,circulatory parts are the terms involving the Theodorsens function C(k). The above equations can be rearranged to separate circulatory and noncirculatory parts to give

Where

$$[R] = \begin{bmatrix}0 & -1\\ 0 & b(a + \frac{1}{2})\end{bmatrix} \qquad [S_1] = \begin{bmatrix}0 & 0\\ 1 & b(\frac{1}{2} - a)\end{bmatrix} \qquad [S_2] = \begin{bmatrix}0 & 0\\ 0 & 1\end{bmatrix}$$

And $[M_{nc}]$ and $[B_{nc}]$ are the aerodynamic non-circlatory mass and damping matrices. Theodorsen function C(k) is approximated in Eqs (17) and rewritten in the following form

$$C(k) = 0.5 + \frac{0.0075}{jk + 0455} + \frac{0.10055}{jk + 0.3} \quad (19)$$

If the circulatory parts of the lift and moment equations are treated separately and the Theodorsen Function approximation is written in Laplace form, after some manipulations the circulatory part becomes

$$2\pi\rho Ub\left(0.5 + \frac{c_{11}s + \frac{U}{bc_{22}}}{\frac{b^2}{U^2}S^2 + b\frac{c_{33}}{U}s + c_{44}}\right)[R][S_1]\begin{bmatrix}\dot{h}\\ \dot{\Theta}\end{bmatrix} + U[R][S_2]\begin{bmatrix}h\\ \Theta\end{bmatrix} =$$

$$\pi\rho bU([R][S_1]\begin{bmatrix}\dot{h}\\ \dot{\Theta}\end{bmatrix} + U[R][S_2]\begin{bmatrix}h\\ \Theta\end{bmatrix} +$$

$$2\pi\rho U^2(C_{11} + \frac{U}{b}c_{22})[R]\begin{bmatrix}0\\ (\frac{\dot{h} + b\left(\frac{1}{2} - a\right)\dot{\Theta} + U\Theta}{S^2 + \frac{U}{b}C_{33}s + \frac{U^2}{b^2}C_{44}})\end{bmatrix} \quad (20)$$

From the above equality the effect of the circulatory part to damping and stiffness matrices can be seen. The circulatory damping and circulatory stiffness matrices are

$$[B_c] = \pi\rho bU[R][S_1]\begin{bmatrix}\dot{h}\\ \dot{\Theta}\end{bmatrix}$$

And

$$[K_c]=\pi\rho b^2[R][S_2]\begin{bmatrix}h\\ b\end{bmatrix} \tag{21}$$

the remaining part of the equality can be used to obtain the aerodynamic states. Since the approximation to the Theodorsen function is of 2nd order, there will be two aerodynamic states. The order of approximation defines the additional aerodynamic states added to the total number of states of the system. By defining

$$X_{a.s} = (\frac{\dot{h} + b\left(\frac{1}{2} - a\right) + U\Theta}{S^2 + \frac{U}{b}C_{33}s + \frac{U^2}{b^2}C_{44}})$$

In state space form aerodynamic state equation can be written in time domain as

$$\begin{bmatrix}\dot{X}_{as1}\\ \dot{X}_{as2}\end{bmatrix} = \begin{bmatrix}0 & 0\\ 1 & b(\frac{1}{2} - a)\end{bmatrix}\begin{bmatrix}\dot{h}\\ \dot{\Theta}\end{bmatrix} + \begin{bmatrix}0 & 0\\ 0 & U\end{bmatrix}\begin{bmatrix}h\\ \Theta\end{bmatrix} + \begin{bmatrix}0 & 1\\ -\frac{U^2C_{44}}{b^2} & -\frac{UC_{33}}{b}\end{bmatrix}\begin{bmatrix}X_{as1}\\ X_{as2}\end{bmatrix} \tag{22}$$

Where $X_{a.s} = X_{as1}$ and $\dot{X}_{as1} = X_{as2}$ and the above equation can be designated by

$$[\dot{X}_{asn}] = [E_1]\begin{bmatrix}h\\ \Theta\end{bmatrix} + [E_2]\begin{bmatrix}\dot{h}\\ \dot{\Theta}\end{bmatrix} + [F]\begin{bmatrix}X_{as1}\\ X_{as2}\end{bmatrix} \tag{23}$$

where n=1,2 , Eqs (20) becomes

$$[B_C]\begin{bmatrix}\dot{h}\\ \dot{\Theta}\end{bmatrix} + [K_C]\begin{bmatrix}h\\ \Theta\end{bmatrix} + 2\pi\rho U^2[R]\left(C_{11}s + \frac{UC_{22}}{b}\right)\begin{bmatrix}0\\ X_{as1}\end{bmatrix} =$$

$$[B_C]\begin{bmatrix}\dot{h}\\ \dot{\Theta}\end{bmatrix} + [K_C]\begin{bmatrix}h\\ \Theta\end{bmatrix} + [D]\begin{bmatrix}X_{as1}\\ \dot{X}_{as1}\end{bmatrix} \tag{24}$$

Where

$$[D] = 2\pi\rho U^2[R]\left(C_{11}s + \frac{UC_{22}}{b}\right)\begin{bmatrix}0\\ X_{as1}\end{bmatrix} = \quad 2\pi\rho U^2[R]\begin{bmatrix}0 & 0\\ \frac{U}{b}C_{22} & C_{11}\end{bmatrix}\begin{bmatrix}X_{as1}\\ \dot{X}_{as1}\end{bmatrix}$$

Writing the equations of motion of the system again with the above manipulations, Eqs 4.1 can be written as

$$[[M] - [M_{nc}]]\begin{bmatrix}\ddot{h}\\ \ddot{\Theta}\end{bmatrix} + [-[B_{nc}] - [B_C]]\begin{bmatrix}\dot{h}\\ \dot{\Theta}\end{bmatrix} + [[K] - [K_C]]\begin{bmatrix}h\\ \Theta\end{bmatrix} = [D]\begin{bmatrix}X_{as1}\\ \dot{X}_{as1}\end{bmatrix} \tag{25}$$

Nonlinear Aeroelastic Equations in Unsteady Flow

Since our aim is to find the flutter boundary of nonlinearities of aeroelastic problems of our model. We need to extend the steady flow problem to unsteady flow problems. Non-intrusive adaptive stochastic collocation method was employed to predict limit-cycle oscillations of an elastically mounted airfoil with random structural properties [23]. On the other approach, a computational method for flutter prediction of turbomachinery cascades were also presented [25]. Non-linearities of transonic flows on a two-degree-of-freedom NACA-64010 airfoil were presented investigated by means of the coupling of a flow solver with a structure solver [15]. So the nonlinearities response can be studied in unsteady flow by adding the nonlinearities of structural part of Eqs. (12) to left side of Esq. (25) and rearrange the problems to the appropriate state space form.

The equation of motion for nonlinear problem could be set as:

$$[[M]-[M_{nc}]]\begin{bmatrix}\ddot{h}\\ \ddot{\Theta}\end{bmatrix}+[-[B_{nc}]-[B_C]]\begin{bmatrix}\dot{h}\\ \dot{\Theta}\end{bmatrix}+[[K]-[K_C]]\begin{bmatrix}h\\ \Theta\end{bmatrix}+[C]\begin{bmatrix}\xi h^4\\ \eta\Theta^4\end{bmatrix}=[D]\begin{bmatrix}X_{as1}\\ \dot{X}_{as1}\end{bmatrix} \tag{26}$$

Here it is possible to designate the parameters in Esq. (26) to simplified expression form as follows.

$$[M_{tot}]=[[M]-[M_{nc}]]$$

$$[B_{tot}]=[-[B_{nc}]-[B_C]]$$

$$[K_{tot}]=[[K]-[K_C]]$$

Where $[C]$ is linear stiffness matrix ,i.e $[C]=[k_h;k_\Theta]$, and ξ and η are the coefficients of Lagrange's equations for nonlinearties of stiffness matrix. Mass, damping and stiffness matrices and the aerodynamic state equations for the whole system can be written as

$$XX1=q \quad XX2=\dot{q} \quad XX3=X_{as1}$$

$$XX2=\ddot{q}=-[M_{tot}]^{-1}[B_{tot}]\dot{q}-[M_{tot}]^{-1}[K_{tot}]q+[M_{tot}]^{-1}[D][X_{asn}]-{M_{tot}}^{-1}[CC] \tag{27}$$

Where $=[h;]$, $[CC]=[C][\xi h^4;\eta\Theta^4]'$ and n = 1, 2

Now we could apply the Runge-kutta solver to find solutions response of system equations. In the following section we are going to simulate the problems by giving initial conditions and increasing the velocities into the systems. Mode shapes have been also analyzed in the simulation of our nonlinearities of aeroelastic problems. Since we are to simulate a number of conditions we need to better select designated cases as shown bellow.

Here you consider cases for simulating step by step initial conditions of unsteady flow in our problems. The structural nonlinearity of the system is common to all of the cases used in our models. We can say,

Case unsteady flow (a) is for unsteady flow with initial conditions of 0 meter and 0.26 rad

Constraints case unsteady flow (b) is for unsteady flow with initial condition of 0.01 meter and 0 rad constraints

Simulations Done and Discussion on Nonlinear Structural Stiffness in Unsteady Flow

In our nonlinear problems we used time domain solution method. Here we are also applying this method in solving the LCO and FFT of the different initial conditions for our model used in equation Eqs (27). Meitour, Lucor and Chassaing [22] addressed the mathematical intersection of the p-method, initial state conditions, and time-domain transformations. The mode shapes, amplitude of frequencies, and convergence or divergence properties have been taken to be considered to study the response of the problems before and after the flutter speed.

Simulation done using the initial condition of 0 m plunge and 0.26 rad pitch

Here flutter speed will be decreased to 0.1m/s. The related dominant two frequencies have been observed during the onset of flutter speed of the simulation result. This happen in the two modes of plunge and pitch motion. The result shows also the excitation frequencies are 1.7 and 4.8 HZ. And they were a bit far from each other.

We have tested the behavior of LCO at the final bound of the flutter zone. The result shows that the 4.8Hz frequency will dominant the 1.7Hz signal by magnitude of amplitude. Here we could observe that 1.7Hz frequency would decrease its amplitude while the 4.8Hz amplitude will gain its amplitude. The mode shape of the two signals are also similar to each other. This could be analyzed in Figure 16b and Figure 16d.

The simulation that are given in the Figure 16-a and Figure 16-c shows that the motion of the plunge and the pitch starts to diverge its motion at 0 sec upto 134 sec in flutter boundary . Here the simulation has to be observed in this time to show that the systems coupling effect will be observed at specified time latter, before completing the whole integration time. Here the coupling of frequency will be observed mostly at the final time of the system flutter zone. This is shown in the Figure 16b and Figure 16d where coupling of the two frequencies pronounced.

Taking the time interval of flutter speed and simulating the system at a velocity bellow flutter speed, LCO will give periodic motion. This shows that there was no sign of coupling frequency at air stream velocity which is less than flutter speed. So in dealing with the flutter speed, generally we should consider:

1. The final bound of the system where coupling is more.

2. Structural undamped case.

3. Simulation test in the flutter zone to find the coupling of the frequencies and maximum FFT amplitude result.

Simulation done using the initial condition of 0.01m plunge and 0 rad pitch

The system has been tested using the above given initial conditions. And the result shows that the flutter speed is at 0.1 m/s. And the time bound has gone till 75 sec. The low speed result shows that there is additional damping action in the system due to aerodynamic forces into the system. The simulations result of the LCO of the two motions showed that the shapes of the two oscillations were different. The excitation frequencies at the flutter speed are 5Hz and 1.7Hz which are similar to the previous case of unsteady flow shown in Figure 16.

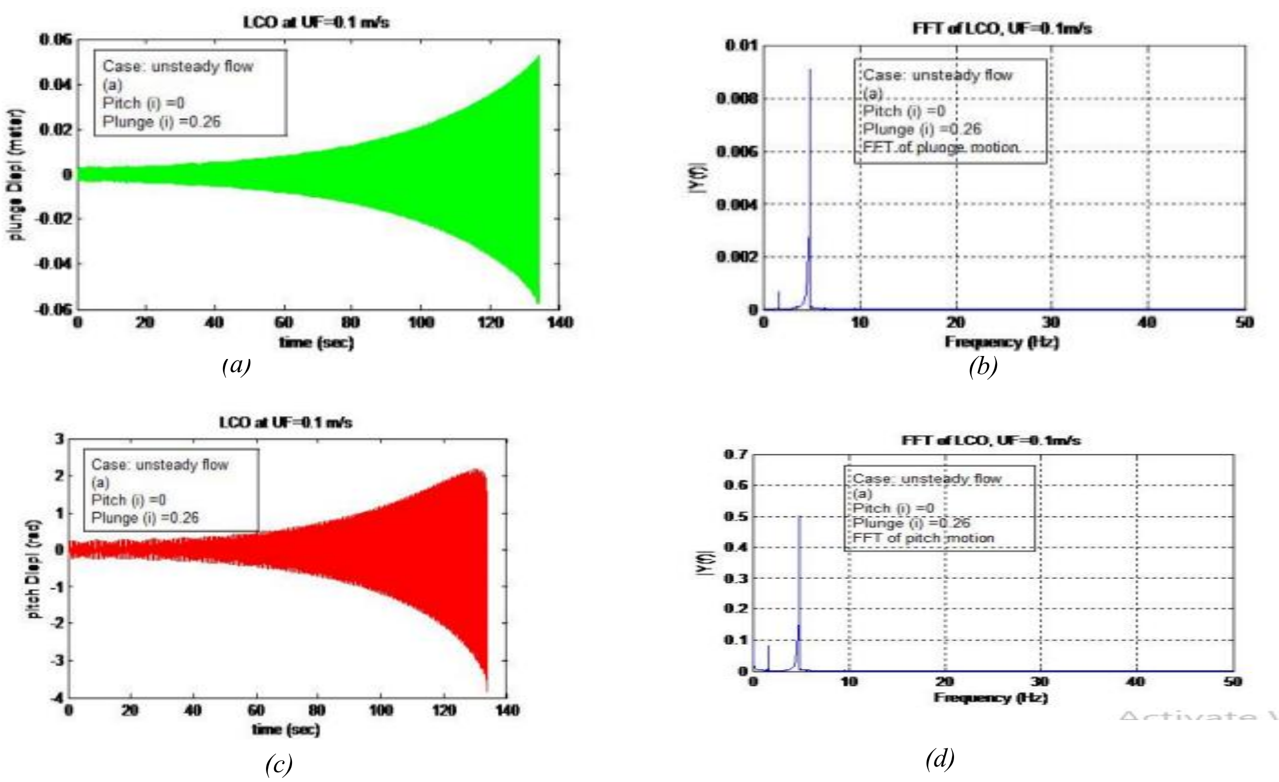

(a) (b)

(c) (d)

Figure 16 Limit cycle of plunge (a), FFT of plunge (b), Limit cycle pitch(c),and FFT of pitch(d) values of nonlinearties stiffness at 0 m plunge and 0.26 rad pitch through unsteady flow

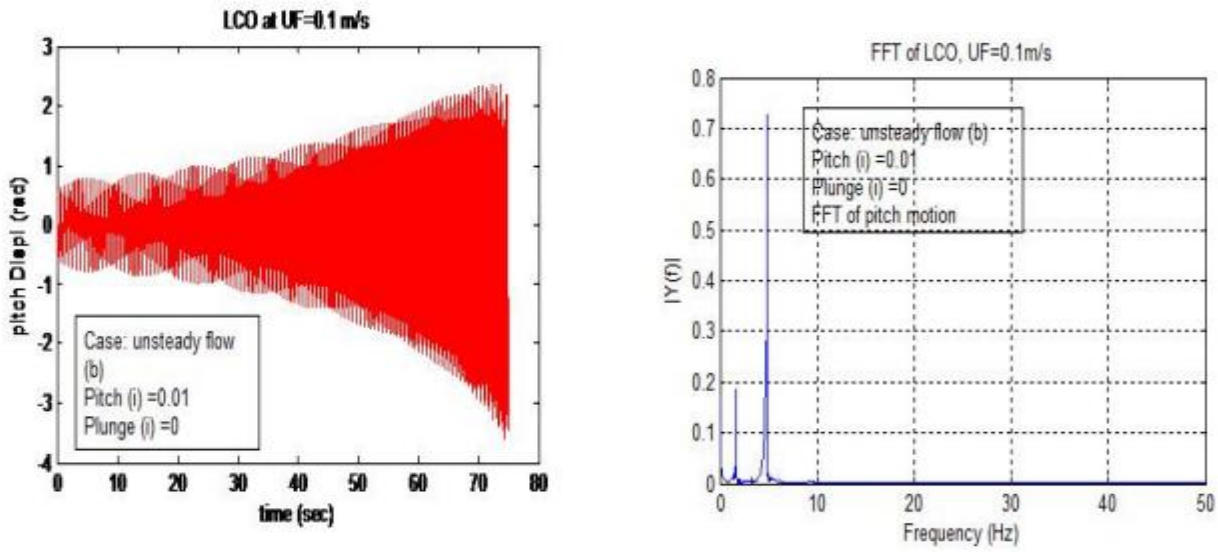

(a) (b)

Figure 18 Limit cycle (a) and FFT (b) values of nonlinearties stiffness at 0.01 m plunge and 0 rad pitch through unsteady flow

The test conducted at the onset of the flutter zone shows that the two frequencies have significant amplitude. This shows that the systems were not in coupling mode. Figure 17a shows the pitch shape of LCO result. And at the same time Figure 17b shows more coupling systems at 75 sec running time of flutter zone. The two peak frequency values of the system are recorded at 1.7 Hz and 4.8 Hz. At the final values of flutter zone the 4.8 Hz frequency value will have more amplitude. So coupling effect is more observed. The periodic motion of the system before the flutter speed is observed in the systems also. The shape of the pitch and the plunge mode could be analyzed from Figure 17a. The frequency versus amplitude figure shows also that shape of the plunge and the pitch signal are different. Here the system needs to be studied more to predict the flutter speed is exactly related to the unsteady flow effect on the airfoil.

The Table 4 summarize what we have seen in the last two cases of the structural nonlinearities through unsteady flow.

Table 4 Summery on nonlinear stiffnesses for the given initial condtions through unsteady flow

<table>
<tr><th rowspan="2">Case</th><th rowspan="2">Range Of Flutter</th><th colspan="2">Mass Effect</th><th colspan="2">Initial Condition</th><th rowspan="2">Flutter Speed
M/S</th><th rowspan="2">Excitation Frequency
HZ</th><th rowspan="2">Convergence</th><th rowspan="2">Coupling Of Frequency</th><th rowspan="2">Amplitude</th></tr>
<tr><th>Plunge
Kg</th><th>Pitch
Kg</th><th>Plunge
m</th><th>Pitch
rad</th></tr>
<tr><td rowspan="2">Figure 16</td><td>$U < U_F$</td><td rowspan="2">10.3</td><td rowspan="2">1.662</td><td rowspan="2">0</td><td rowspan="2">0.26</td><td rowspan="2">0.1</td><td rowspan="2">1.7,4.8</td><td>Periodic</td><td>Small</td><td rowspan="2">4.3</td></tr>
<tr><td>$U > U_F$</td><td>Diverge</td><td>High</td></tr>
<tr><td rowspan="2">Figure 17</td><td>$U < U_F$</td><td rowspan="2">10.3</td><td rowspan="2">1.662</td><td rowspan="2">0.01</td><td rowspan="2">0</td><td rowspan="2">0.1</td><td rowspan="2">1.7,4.8</td><td>Periodic</td><td>Small</td><td rowspan="2">13.8</td></tr>
<tr><td>$U > U_F$</td><td>Diverge</td><td>High</td></tr>
</table>

6 CONCLUSIONS

This paper is tried to see aeroelastic stability of nonlinearities of plunge and pitch stiffness in steady and unsteady flow. No structural damping action has been involved in this model. The problem statements of this paper are mainly to find stability of the cubic nonlinearities of stiffness of aeroelastic problem and compare the results with the linear solution output. Mainly three areas of simulation output have been conducted in these aeroelastic problems.

1. Structural linear stiffness through steady flow
2. Nonlinear structural stiffness through steady flow
3. Nonlinear structural stiffness through unsteady flow

Aerodynamically, analytical derivation has been taken for steady and unsteady flow theory. For steady flow the coefficient slop is taken as 2π and for unsteady flow case, concept of Theodorsen's Unsteady Thin-airfoil theory has been considered.

The time marching solution method has been used in simulating our aeroelastic problems. The smallest time span interval taken for integrating is 0.01 second.

Selected plunge and pitch initial constraints have been conducted to study behavior of each constraint to one another. The selected initial conditions for each of the configuration is given as follows

1. 0 m plunge constraints and 0.26 rad pitch constraints
2.0.01 m plunge constraints and 0 rad pitch constraints
3. The same mass effect for 0.01 and 0 rad constraints

In the case of structural linear aeroelastic analysis, the result shows that

1. The frequencies are coupled in all the given three initial conditions.
2. Amplitude is dependent on the given initial condition.
3. For the same mass effect the flutter velocities has increased.
4. The excitation frequency is 2.5.

In the case of structural nonlinear stiffness in steady flow

1. One dominant amplitude frequency value will be observed in the flutter zone.
2. There could be coupling phenomenon at the start of flutter zone. But two peak frequencies may be observed at the final bound of the flutter zone. The instabilities has increased at the flutter zone may be due to the existence of a number of amplitude in the flutter zone. The range of the two peak frequencies are between 2 and 2.6 at the flutter zone.
3. Flutter speed is less than that of the linear problem if you are taking and compare the same initial condition cases. 4. By taking nonzero constraints of plunge and pitch in these nonlinear stiffness problems, we could see that the flutter speed has decreased to 5.4 m/s.

In the cases of structural nonlinear stiffness in unsteady flow

1. The two excitation frequencies are 4.8Hz and 1.7Hz.
2. The simulation result shows that the 4.8 Hz signal will dominate the other frequencies
at the time of flutter zone comes into action in the case unsteady (a). This has been also observed in the case unsteady flow (b). At the time of flutter speed, single frequency amplitude of 4.8 HZ will have peak amplitude than the 1.7Hz. Besides the amplitude at 1.7 will decreased from the first possessed amplitude.

From the work we presented in this paper, general conclusions may be drawn.

1. The flutter speed varies depending on structural nonlinearities with its initial conditions of plunge and pitch stiffness set.
2. The plunge nonlinear stability effects is dominant than pitch initial effects so that the system will be liable to flutter zone easily with advancing of plunge initial conditions.
3. The Unsteady flow will have positive impact on reducing early creation of flutter zone on aroelastic systems.
4. The summing effect of the initial conditions on the system could cause decreasing of flutter speed.
5. In the flutter zone, you may face the coupling and less coupling of frequencies in the system.
6. For the same mass effect the flutter velocities have increased.

Future Scope

The continuation of the project will focus on

1. Experimental work that will be conducted to validate the response of the systems with analytical values.
2. Damping action that will be included in the structural member.
3. Extending the aeroelastic stability for more number of degree freedom systems will be considered.

ACKNOWLEDGEMENT

Firstly I would like to thank my guide DR. S.S.Gupta who has provided me with guidance and assistance through this project. So it has been a great privilege for me to work with him.

I would also like to thank my co-supervisor Sunil Nimje who has helped me by facilitating the research work and giving proper guide to finalize the research work. I am greatly acknowledge the inspiration and co-operation from assistance prof. C.S Dharankas for helping me to know the insight of the problems by giving his time if discussion has needed.

I wish also to express my gratitude to Dr. S.Talole, Head Department of Aerospace Engineering who has taught me Latex format which I used it for this research paper at Pune, India.

I would like also to thank the staff of CAD-CAM lab for all the helped they provided me facilitated environment to work with it. Kindly I gratefully thank staff of aerospace engineering department who have made fun and cooperative environment throughout my contact time. Finally I would like to thanks friends and my family who are always with me.

REFERENCES

[1] .T. O'Neil and T. Strganac, "Aeroelastic response of a rigid wing supported by nonlinear springs," Journal of Aircraft, vol. 35, no. 4, pp. 616-622, 1998, doi: doi.org/10.2514/2.2345.

[2] .D. H. Hodges and Pierce, G. A., Introduction to structural dynamics and aeroelasticity, vol. 15, cambridge university press, 2011.

[3] .S. T. Trickey, Virgin, L. N. and Dowell, E. H., "The stability of limit–cycle oscillations in a nonlinear aeroelastic system," in Proceedings of the Royal Society of London. Series A: Mathematical, Physical and Engineering Sciences, 2002, doi:doi.org/10.1098/rspa.2002.0965.

[4] .J. J. Block and Strganac, T. W., "Applied active control for a nonlinear aeroelastic structure," Journal of Guidance, Control, and Dynamics, vol. 21, no. 6, pp. 838-845, 1998, doi:doi.org/10.2514/2.4346.

[5] .C. M. P. &. B. E. Rubillo, P. Marzocca and E. Bollt, "Active aeroelastic control of lifting surfaces via jet reaction limiter control," International Journal of Bifurcation and Chaos, vol. 16, no. 09, pp. 2559-2574, 2006, doi:doi.org/10.1142/S0218127406016252.

[6] .N. M. , M. K. and F. C. , "Coupled analytical sensitivity analysis and optimization of three-dimensional nonlinear aeroelastic systems," AIAA journal, vol. 39, no. 11, pp. 2051-2061, 2001, doi:doi.org/10.2514/2.1227.

[7] .B. H. K. Lee, L. Liu and Y. S. Wong, "Limit-cycle oscillations of an airfoil with piece-wise linear restoring forces," in In Proc. ICAS 2002 Congress, 2002.

[8] .L. Liu and Dowell, E. H. , "The secondary bifurcation of an aeroelastic airfoil motion: effect of high harmonics," Nonlinear Dynamics, vol. 37, no. 1, pp. 31-49, 2004.

[9] .B. H. K. Lee, Price, S. J. and Wong, Y. S. , "Nonlinear aeroelastic analysis of airfoils: bifurcation and chaos," Progress in aerospace sciences, vol. 35), no. 3, pp. 205-334, 1999, doi:doi.org/10.1016/S0376-0421(98)00015-3.

[10] .Sarkar, S. and Bijl, H. , "Nonlinear Aeroelastic Study of Stall Induced Oscillation in a Symmetric Airfoil," in In ECCOMAS CFD 2006: Proceedings of the European Conference on Computational Fluid Dynamics,September 5-8, 2006, Egmond aan Zee, The Netherlands, September, 2006, http://www.lr.tudelft.nl/aerodynamics.

[11] .C. D. M. Junior, R. Daniela C. , M. B. Eduardo and D. M. Flávio , "Identification of flutter parameters for a wing model," Journal of the Brazilian Society of Mechanical Sciences and Engineering, vol. 28, pp. 339-346., 2006, doi:doi.org/10.1590/S1678-58782006000300012.

[12].L. Meirovitch, Fundamentals of vibrations, Waveland Press., 2011.

[13].S. U. Ünal, "Design, Construction And Preliminary Testin of an Aeroservoelastic Test Apparatus to be Used in Ankara Wind Tunnel (Master's thesis, Middle East Technical University (Turkey))," 2005.

[14].J. Anderson, EBOOK: Fundamentals of Aerodynamics (SI units), McGraw hill, 2011.

[15].J. Bohbot, Garnier, J., Toumit, S. and Darracq, D., "Computation of the flutter boundary of an airfoil with a parallel Navier-Stokes solver," in In 39th Aerospace Sciences Meeting and Exhibit, 2012, doi:doi.org/10.2514/6.2001-572.

[16].R. L. Bisplinghoff and Ashley, H., Principles of aeroelasticity, Courier Corporation, 2013.

[17].E. H. Dowell, A modern course in aeroelasticity, vol. 34, MECCANICA-MILANO-34: 140-140, 1999, pp. 140-140.

[18].J. Alonso and Jameson, A., "Fully-implicit time-marching aeroelastic solutions," in In 32nd Aerospace Sciences Meeting and Exhibit, 1994, January, doi:doi/abs/10.2514/6.1994-56.

[19].L. Zhu, Xie, C., An, C. and Man, S., "Nonlinear aeroelastic analysis of airfoils using a continuous-time state-space panel method with viscous effects," Physics of Fluids, vol. 37, no. 8, 2025, doi:doi.org/10.1063/5.0285151.

[20].T. S. R. Reddy, Srivastava, R. and Mehmed, O., "Flutter and Forced Response Analyses of Cascades Using a Two-Dimensional Linearized Euler Solver," 1999, ntrs.nasa.gov/citations/20000024921.

[21].Z. Jian and Jinwu, X., "Nonlinear aeroelastic response of high-aspect-ratio flexible wings," chinese Journal of Aeronautics, vol. 22, no. 4, pp. 355-363, 2009, doi:doi.org/10.1016/S1000-9361(08)60111-9.

[22].M. H. Kargarnovin and Mamandi, A., "Aeroelastic response for pure plunging motion of a typical section due to sharp edged gust, using Jones approximation aerodynamics.," World Academy of Science, vol. 36, no. 1, pp. 154-161, 2007.

[23].J. Le Meitour, J., Lucor, D. and Chassaing, J. C., "Prediction of stochastic limit cycle oscillations using an adaptive polynomial chaos method," Journal of

Aeroelasticity and Structural Dynamics, vol. 2, no. 1, 2010, doi: doi:10.3293/asdj.2010.

[24].M. Ghommem, Nayfeh, A. H. and Hajj, M. R., "Control of Limit Cycle Oscillations of a Two-Dimensional Aeroelastic System," Mathematical Problems in Engineering, vol. 2010(1), 782457, 2010, doi:doi.org/10.1155/2010/782457

[25].M. Sadeghi and Liu, F. , "Computation of cascade flutter by uncoupled and coupled methods," International Journal of Computational Fluid Dynamics, vol. 19, no. 8, pp. 559-569, 2005, doi.org/10.1080/10618560500508367.